



Geophysical Research Letters

Supporting Information for

Drought-induced vertical displacements and water loss in the Po river basin (Northern Italy) from GNSS measurements

F. Pintori¹ and E. Serpelloni¹

¹Istituto Nazionale di Geofisica e Vulcanologia (INGV), Bologna, 40128, Italy.

Contents of this file

Text S1
Figures S1 to S9

Introduction

We provide additional figures to better explain how the time series are analyzed. These figures also support the inversion strategy employed to estimate the terrestrial water storage variations and what is presented in the discussion. Furthermore, Text S1 provides a detailed description of the checkerboard tests used to determine the spatial resolution of the terrestrial water storage variations.

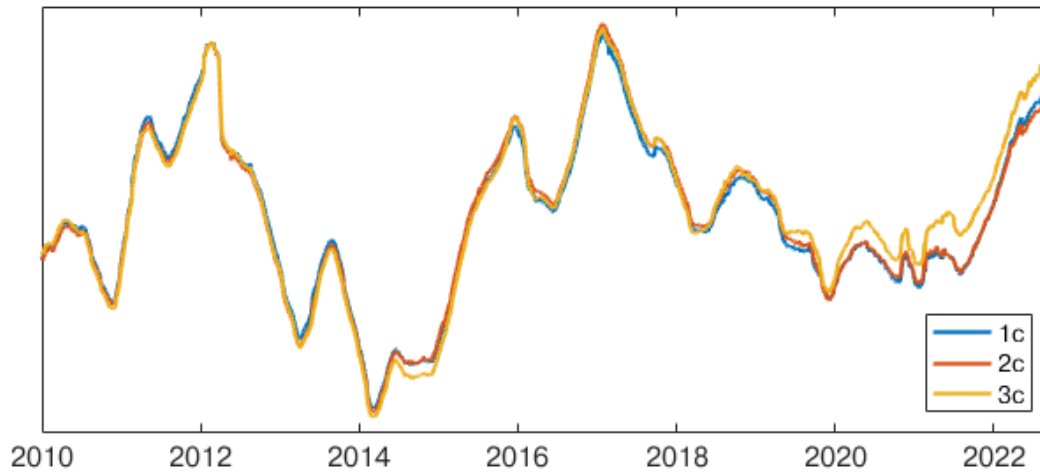


Figure S1. Comparison of the temporal evolution of the PC1 obtained considering 1 (blue), 2 (red) and 3 (yellow) total principal components.

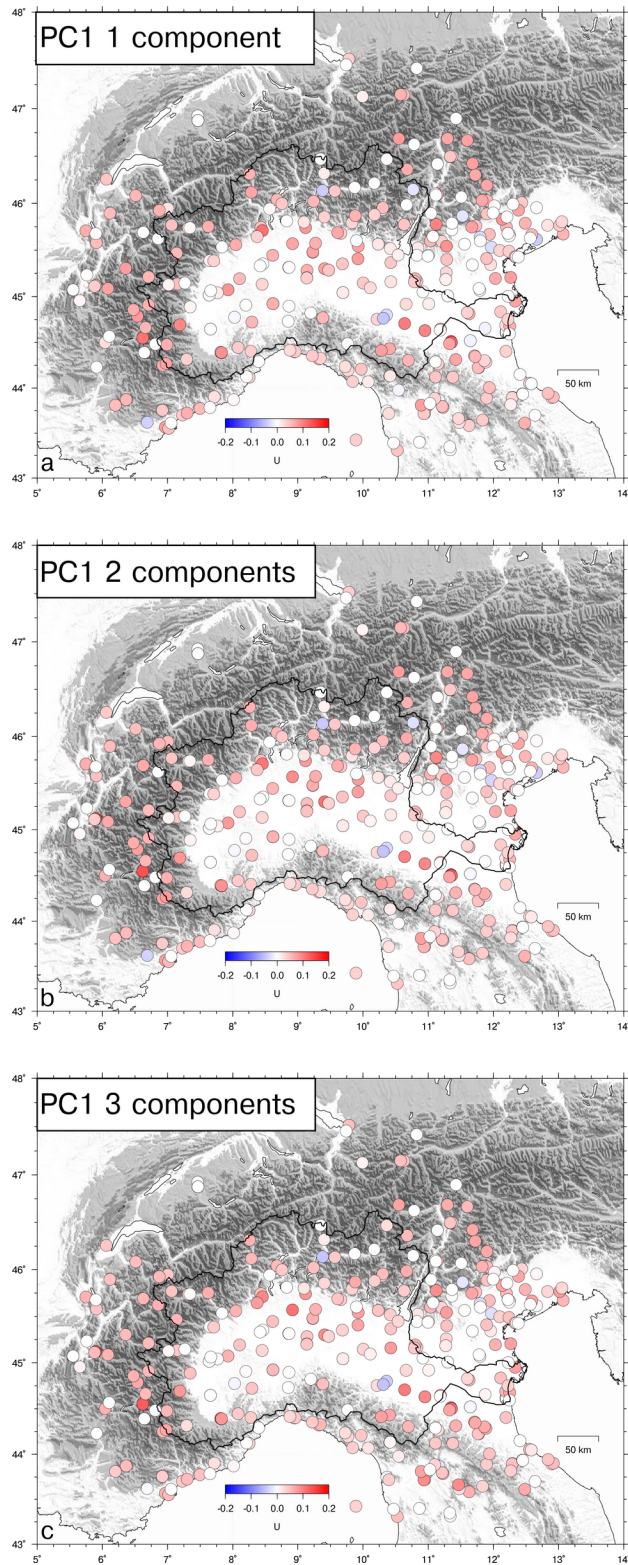


Figure S2. Comparison of the spatial responses of the PC1 obtained considering 1 (a), 2 (b) and 3 (c) total principal components.

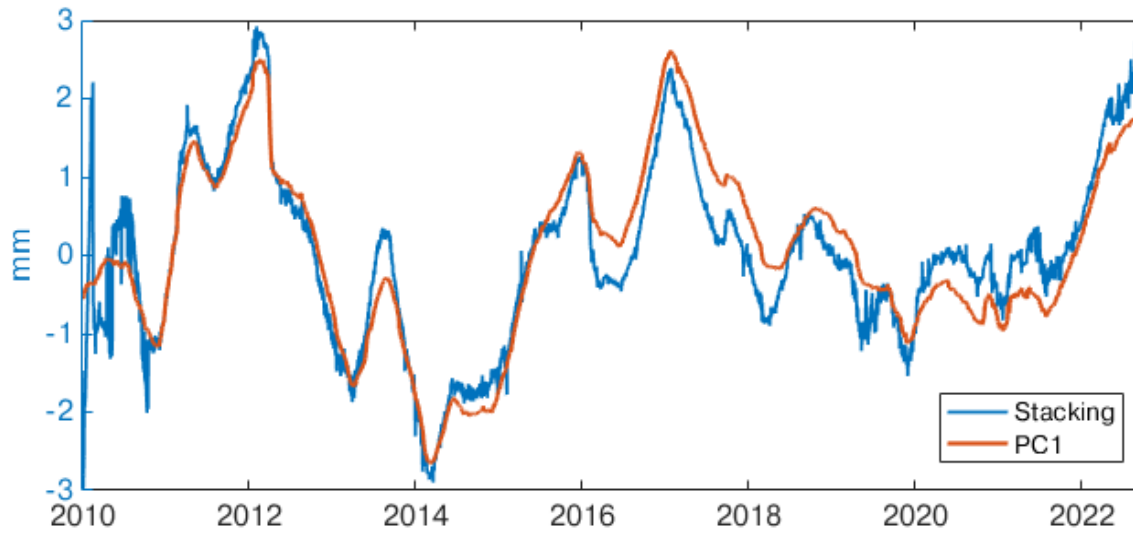


Figure S3. Comparison of the temporal evolution of the PC1 (red) with the common mode signal of the network obtained by performing a weighted stacking (blue).

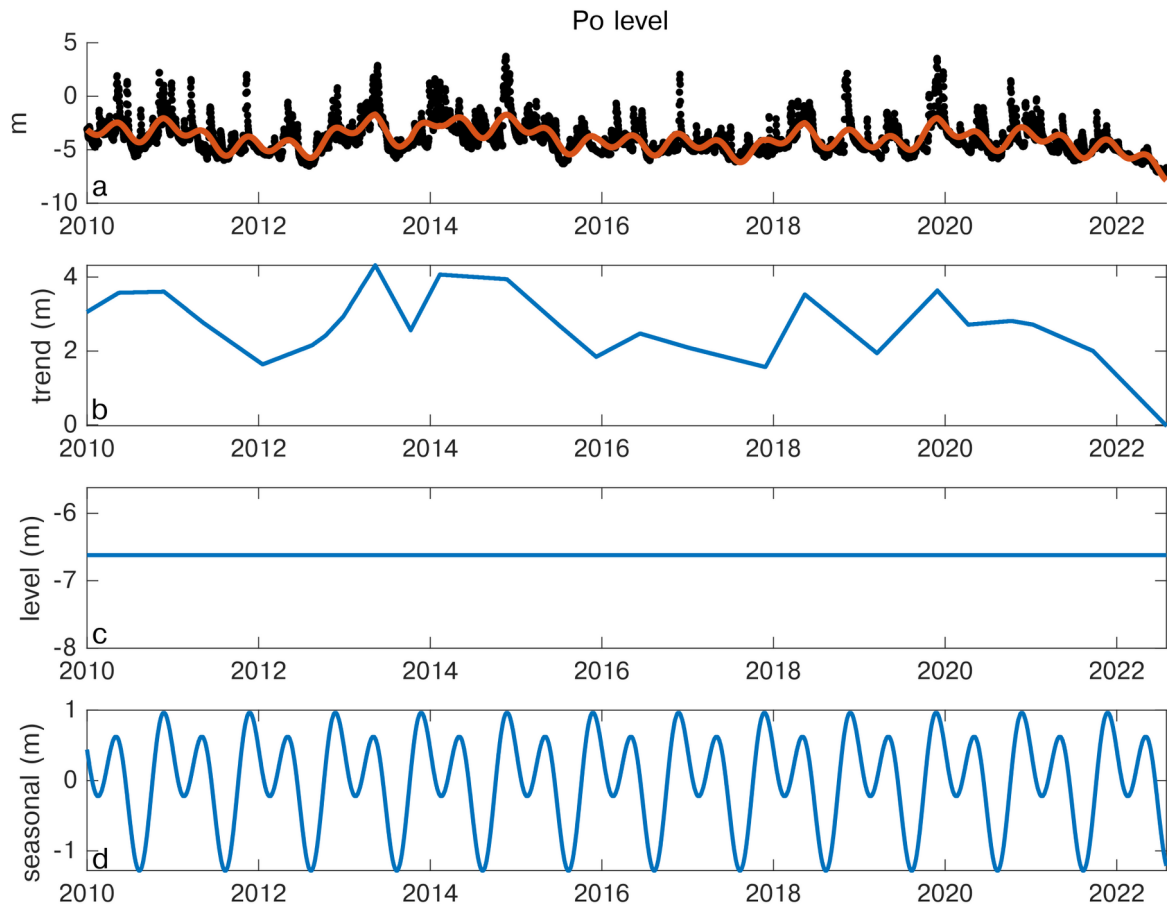


Figure S4. Decomposition of the Po river level measurements, performed using the L1 tool software. In a) the black dots represent the original time series, the red line the L1 tool model, which is the sum of the trend (b), level (c) and seasonal component (d).

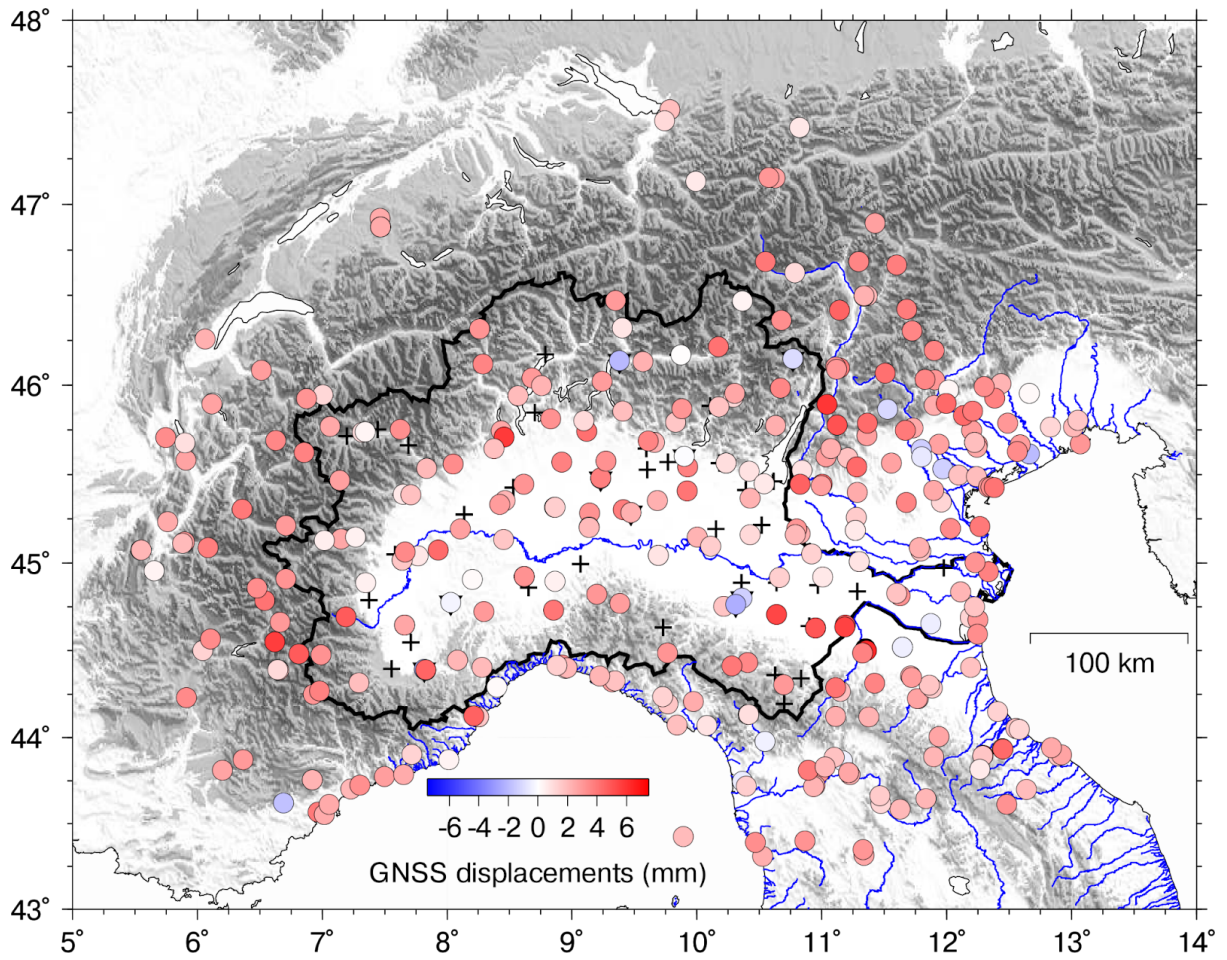


Figure S5. Vertical displacements associated with PC1 during the 2021.00 (January, 2021) - 2022.67 (September, 2022) time interval.

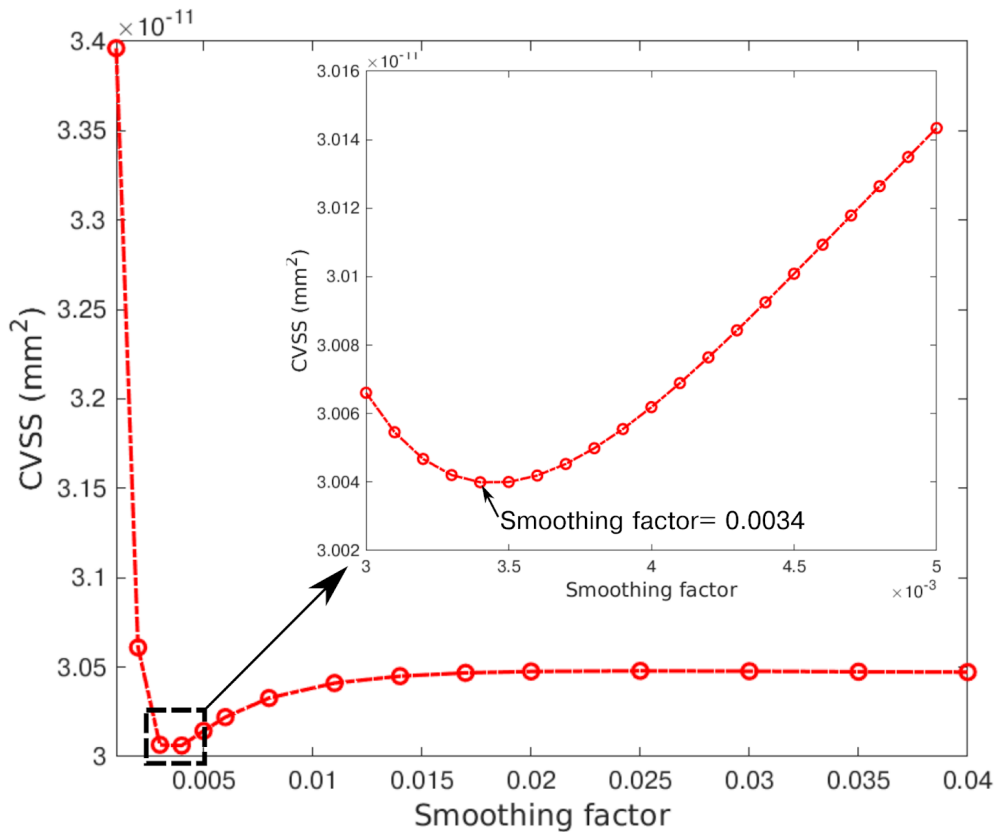


Figure S6. Relation between the sum of squared residuals from cross-validation (CVSS) and the smoothing factor.

Text S1.

A checkerboard test using synthetic inputs is performed to show the ability of the inversion method and the distribution of the GNSS stations to resolve spatial features of water mass variation in a checkerboard pattern, where each mass has dimensions of $1^\circ \times 1^\circ$ and an EWH change of 300 mm (Fig. S7a). The inversion performance is evaluated estimating the agreement dR between each grid point of the checkerboard synthetic model within the Po river basin and the results of the inversion (Fig. S7a) using the following equation, which estimates the percentage of accuracy:

$$dR = 1 - \frac{|input - output|}{\max(input)}$$

where *input* is the value of the checkerboard synthetic model, *output* the value resulting from the inversion and $\max(input)$ the maximum value of *input*, i.e. 300 mm.

The mean value of dR computed over all the grid points is 0.67, then we can conclude that the accuracy of our inversion, at the resolution of $1^\circ \times 1^\circ$, is 67%. By using smaller patches we find a rapid degradation of the spatial accuracy (Fig. S7a-b).

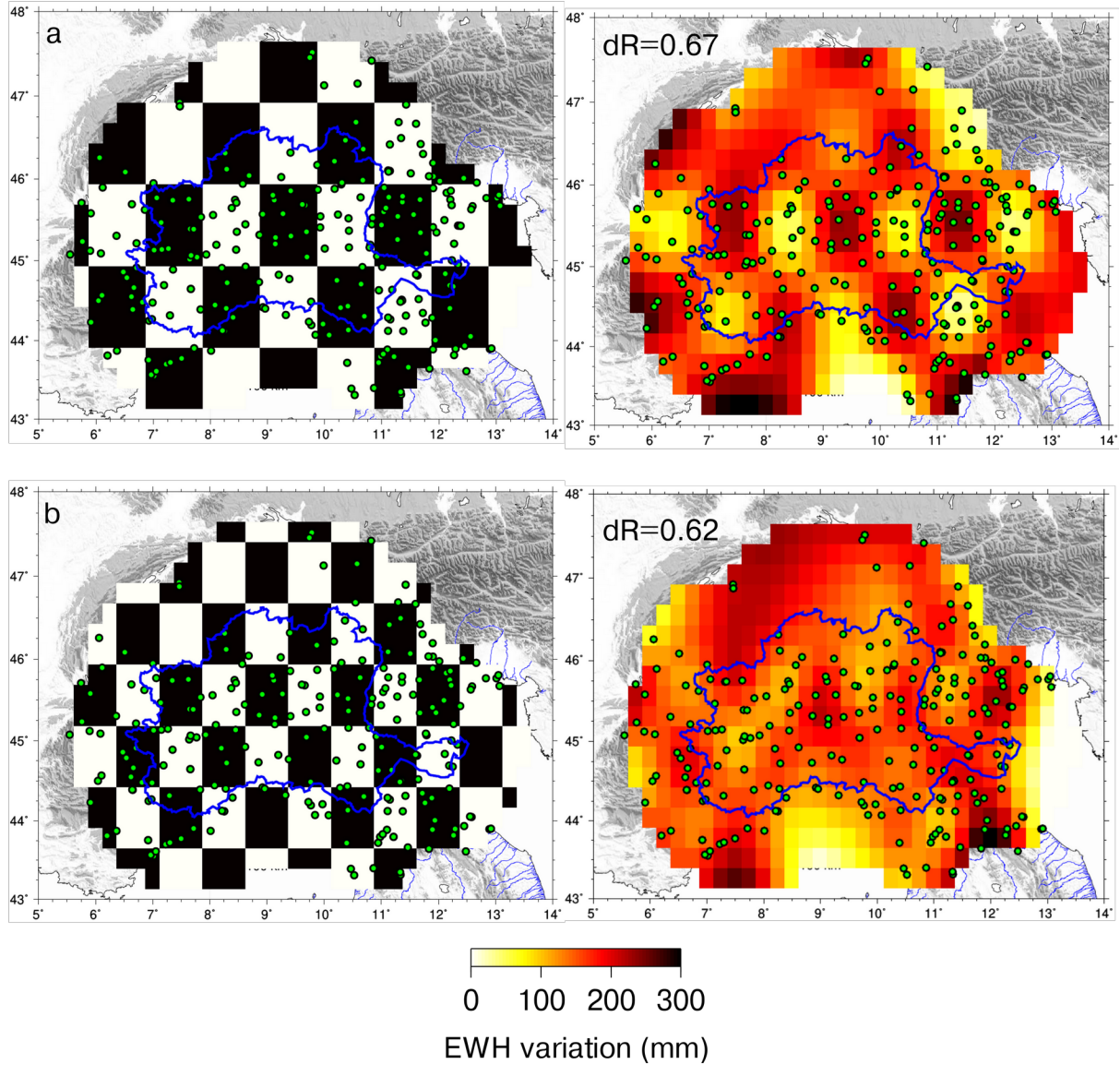


Figure S7. Checkerboard test using synthetic data. a) Comparison between the checkerboard synthetic model (left) and the results using the GNSS2TWS inversion method (right) considering a 1.00° spatial resolution. b) Same as a) but considering a 0.75° spatial resolution.

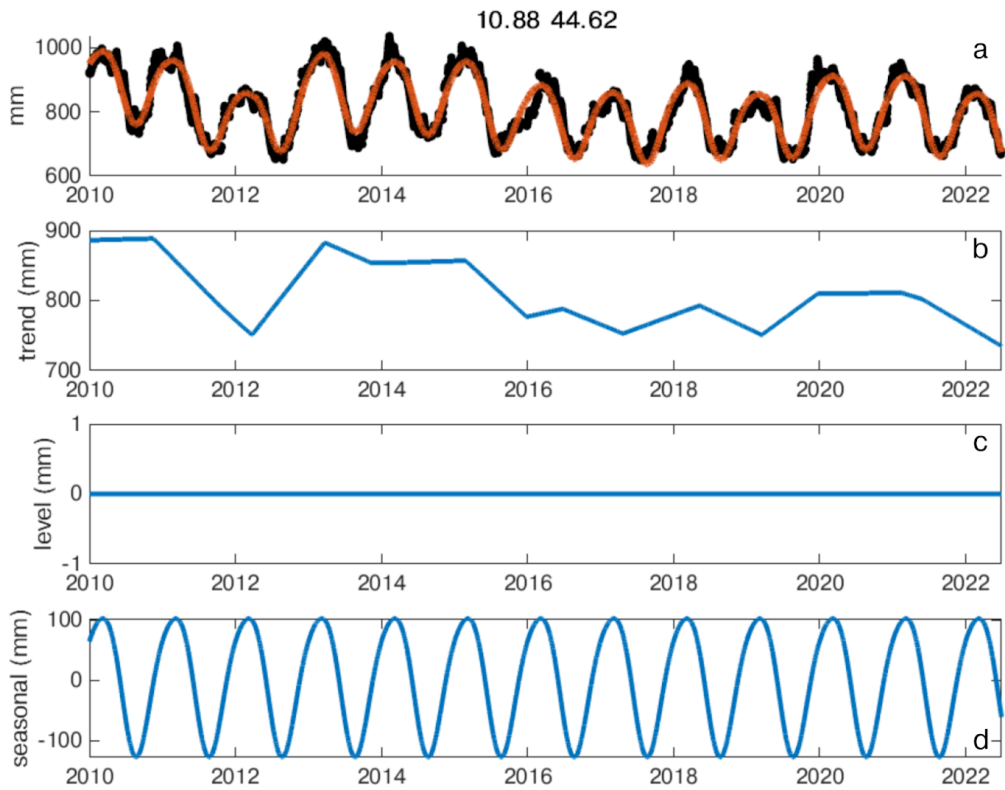


Figure S8. Decomposition of the GLDAS surface water content time series, associated with the cell with coordinates lon= 10.88°, lat= 44.62°, performed using the L1 tool software. In a) the black dots represent the original time series, the red line the L1 tool model, which is the sum of the trend (b), level (c) and seasonal component (d).

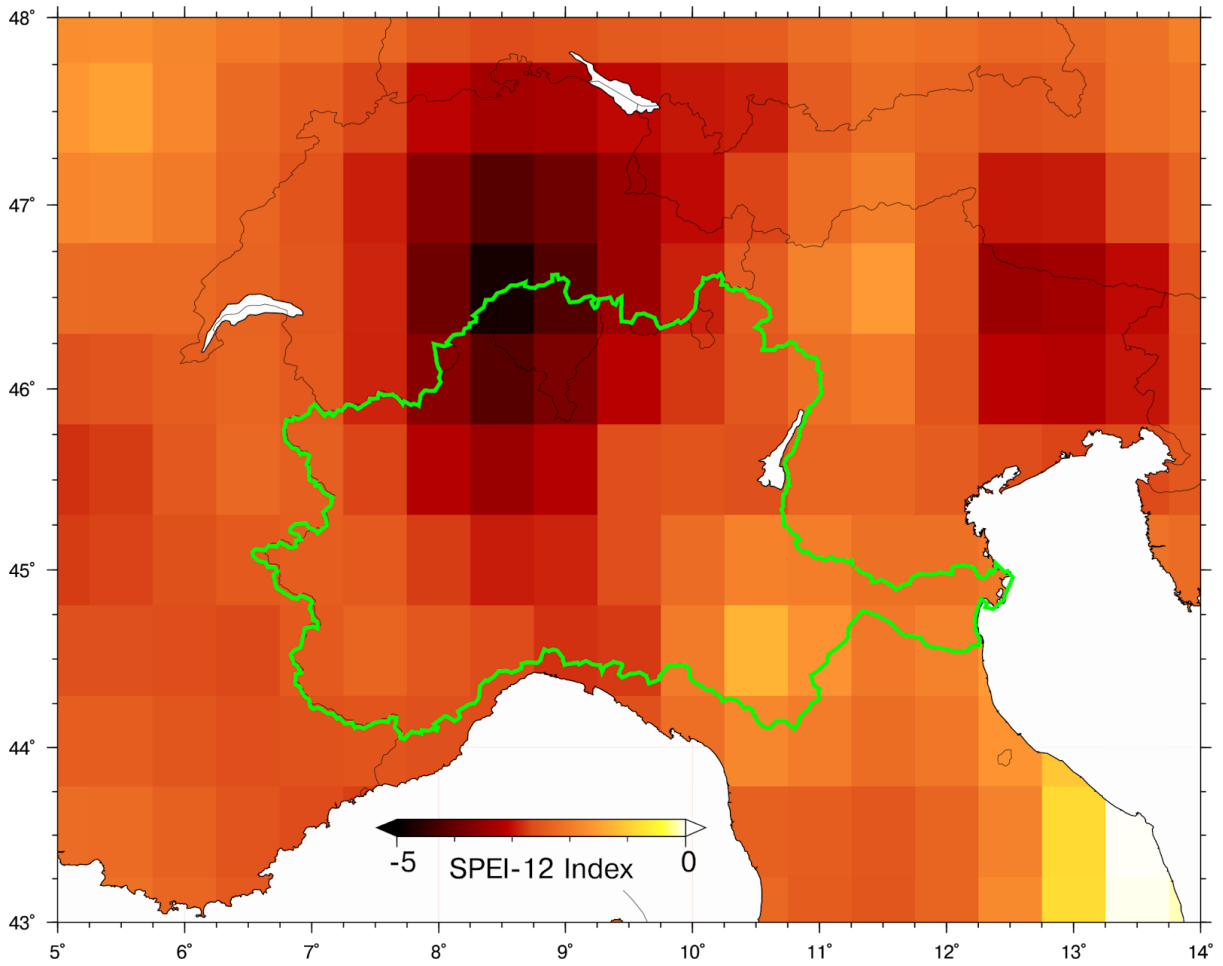


Figure S9. Zoom of the SPEI-12 maps, computed in August 2022, shown in Fig.1, considering only the negative values and the same color palette of Fig. 4.